Sensitivity of the SHiP experiment to Dark Photons

The SHiP collaboration

March 12, 2019

Abstract

Dark photons are hypothetical vector particles that could act as mediators between the standard model particles and a hidden sector. The simplest of such vector-portal models is fully characterised by only two parameters: the mass of the dark photon m_{γ_D} and its mixing parameter with the photon, ε. The sensitivity of the SHiP detector is reviewed for dark photons in the mass range between 0.01 and 10 GeV. Different production mechanisms are simulated, with the dark photons decaying to pairs of visible fermions. Exclusion contours are presented and compared with those of other existing or planned experiments. The SHiP detector is expected to have a unique sensitivity for m_{γ_D} ranging between XX and XX GeV, and ε ranging between XX and XX.

Contents

1 Introduction

The CERN beam facility located near Geneva, Switzerland, comprises several particle accelerators among which the Large Hadron Collider (LHC) [1] is the World's largest and most energetic to date. High-energy protons are delivered to the LHC by the Super Proton Synchrotron (SPS). The 400-GeV proton beam of the SPS is also used in fixed-target experiments. The LHC is planned to be upgraded into a High-Luminosity machine around 2025 with the HL-LHC program [2].

In parallel to the high-energy frontier probed by the LHC, another complementary way of exploring the phase space to find new physics is through the "intensity frontier". By probing lower-energy scenarios, the aim is to identify whether the new physics could be hidden from sight due to weak connections through portals instead of direct interactions with the known particles, with the new particles living in a hidden sector. The simplest extensions of the standard model (SM) are possible through three types of portals, involving either a scalar (e.g. dark Higgs boson), a vector (e.g. dark photon) or fermions (e.g. heavy neutral leptons). Strong constraints exist already from the LHC experiments on high-mass short-lived mediators [3, 4, 5, 6]. The long-lived scenarios with relatively low masses remain however largely unexplored. The SHiP (Search for Hidden Particles) experiment[7] has been proposed in 2012 and designed to look for particles which would decay in the range 50-120 m from their production vertices. The sensitivity of the SHiP detector to heavy neutral leptons has been investigated in [8]. This article is dedicated to studying the sensitivity of the SHiP detector to dark photons.

After describing briefly the SHiP detector and its simulation in section 2, the theory considered for the dark photon production and decay is reviewed in section 3. The sensitivity of the SHiP detector is given in section 4 for the three production modes studied and decay to visible fermions, in the minimal dark photon model. Leptophilic scenarios are also considered. Finally section 5 provides a conclusion.

2 The SHiP Detector and Simulation

SHiP[7] is a new general purpose fixed target facility proposed at the CERN SPS accelerator to search for particles predicted by Hidden Portals. These particles are expected to be predominantly accessible through the decays of heavy hadrons. The facility is therefore designed to maximise the production and detector acceptance of charm and beauty mesons, while providing the cleanest possible environment. The 400 GeV proton beam extracted from the SPS will be dumped on a high density target with the aim of accumulating 2×10^{20} protons on target (p.o.t.) during 5 years of operation. The charm production at SHiP exceeds any existing and planned facility.

A dedicated detector, based on a long vacuum tank followed by a spectrometer and particle identification detectors, will allow probing a variety of models with light long-lived exotic particles and masses below $\mathcal{O}(10)$ GeV/c^2. Since the hidden sector particles originating from charm and beauty are produced with a significant transverse momentum with respect to the beam axis, the detector should be placed as close as possible to the target. A critical component of SHiP is the muon shield, which deflects the high flux of muons produced in the target, that would represent a very serious background for the particle searches, away from the detector. The detector is designed to fully reconstruct the exclusive decays of hidden particles and to reject the background down to below 0.1 events in the sample of 2×10^{20} protons on target. The detector consists of a large magnetic spectrometer located downstream of a 50 m-long and 5×10 m-wide decay volume. To suppress the background from neutrinos interacting in the fiducial

volume, the decay volume is maintained under a vacuum. The spectrometer is designed to accurately reconstruct the decay vertex, mass and impact parameter of the decaying particle at the target. A set of calorimeters followed by muon chambers provide identification of electrons, photons, muons and charged hadrons. A dedicated timing detector measures the coincidence of the decay products, which allows the rejection of combinatorial backgrounds. The decay volume is surrounded by background taggers to tag neutrino and muon inelastic scattering in the surrounding structures, which may produce long-lived SM V^0 particles, such as $\mathrm{K_L}$, that have similar topologies to the expected signals.

The experimental facility is also ideally suited for studying interactions of tau neutrinos. It will therefore host an emulsion cloud chamber based on the Opera concept, upstream of the hidden-particle decay volume, followed by a muon spectrometer.

In the simulation, proton fixed target collisions are generated by PYTHIA 8.2 [9], inelastic neutrino interactions by GENIE [10] and inelastic muon interactions by PYTHIA 6 [11]. The heavy flavour cascade production is also taken into account [12]. The SHiP detector response is simulated in the GEANT4 [13] framework. The simulation is done within the FAIRROOT framework [14].

3 Dark photon production mechanisms

The minimal dark photon model considers the addition of a U(1) gauge group to the SM, whose gauge boson is a vector field called the dark photon γ^{D} . A kinetic mixing between the dark photon and the SM U(1) gauge bosons is allowed [15], with a reduced strength parametrised by a coupling ε, also called the kinetic mixing parameter. In its simplest form, the knowledge of the mass of the dark photon $\mathrm{m}_{\gamma^{\mathrm{D}}}$ and the kinetic mixing parameter ε is enough to characterise the model and calculate production cross section and decay properties.

Different mechanisms are possible for the production of such new particles at a fixed-target experiment. Three different modes are studied in this paper.

The initial 400 GeV proton beam interacts with the protons from the target material, producing mesons. For meson decay channels involving photons, there is a possibility for the photon to mix with the dark photon, as described in subsection 3.1 below. This mode is opened only for dark photon masses below 0.9 GeV, as for mesons with masses above this threshold the main decay modes don't involve photons anymore.

The proton-proton interaction could also lead to the radiation of a dark photon via a bremsstrahlung process, as described in subsection 3.2 below. This mode is heavily suppressed when the dark photon mass is heavier than the Quantum Chromodynamic (QCD) scale, so remains competitive only for masses below $\simeq 2$ GeV.

The last production mode studied here is via a Drell-Yan like QCD process, or quark-quark annihilation into the dark photon, as described in subsection 3.3 below. For this to happen, the dark photon mass can be in the 1.4-10 GeV range. Using the parton model with a factorisation scale below the GeV scale cannot give sensible results, as expected from the range of validity of parton distribution functions, and hence this area of phase-space has not been considered here.

In this paper, the assumption that only the initial proton interacts is made. In reality, similar interactions could also happen from protons coming from cascade decays happening in the target material. For electromagnetic processes (electron bremsstrahlung of photons mixing with the dark photon), it has been shown in [16] that their contribution is negligible compared to the main production mechanisms described above. The study however remains to be done for hadronic interactions in the cascade decays, and will be the subject of future work. Hence the results presented here are conservative and the sensitivity could be improved in the future when

this contribution is added.

The dark photon decay to pairs of visible fermions is considered as described in subsection 3.4 below.

3.1 Production in meson decay

The Pythia 8.2 [9] Monte Carlo (MC) generator is used to produce inclusive QCD events in proton-proton collisions, through all available non-diffractive processes. One proton beam momentum is set to 400 GeV and the other to 0 (protons from the fixed target material). The total proton-proton cross section with a corresponding center-of-mass energy of 27.43 GeV is predicted to be $\sigma_{\rm pp}^{\rm tot} = 40.6 \pm 1.2$ mb [17], and the non-diffractive cross section given by Pythia is $\sigma_{\rm pp}^{\rm non-diff} = 24$ mb. The mesons that are produced are then used as sources of dark photons, if they have decay modes to photons and their decay to a dark photon of mass $\rm m_{\gamma^D}$ is kinematically allowed. Four processes are found largely dominant (with other contributions neglected) and shown in table 1. The decay tables of these four mesons are reset to having only one decay mode allowed with 100% branching ratio ($\pi^0 \to \gamma\gamma$, $\eta \to \gamma\gamma$, $\omega \to \pi^0\gamma$, $\eta' \to \gamma\gamma$). If several mesons of interest are produced, only the last one encountered is considered.

The branching ratios of the mesons to these new decay modes are function of the $\rm m_{\gamma^D}$, the mixing parameter ε, the meson type, pseudo-scalar or vector, and the meson mass [18, 16]. For pseudo-scalar mesons $\mathcal{P}$ (π^0, η^0 and η'), the branching ratio to $\gamma^{\rm D}$ γ is given by equation 1. For vector mesons $\mathcal{V}$ (ω), the branching ratio to a $\gamma^{\rm D}$ and a pseudoscalar meson $\mathcal{P}$ is given by equation 2.

$$\mathrm{Br}(\mathcal{P} \to \gamma^{\rm D}\,\gamma) \simeq 2\epsilon^2 \left(1 - \frac{m_{\gamma^{\rm D}}^2}{m_{\mathcal{P}}^2}\right)^3 \mathrm{Br}(\mathcal{P} \to \gamma\gamma)\,, \tag{1}$$

$$\mathrm{Br}(\mathcal{V}^\pm \to \mathcal{P}\gamma^{\rm D}\,) \simeq \epsilon^2 \times \mathrm{Br}(\mathcal{V}^\pm \to \mathcal{P}\gamma) \times \frac{(m_{\mathcal{V}}^2 - m_{\gamma^{\rm D}}^2\ - m_{\mathcal{P}}^2)^2\sqrt{(m_{\mathcal{V}}^2 - m_{\gamma^{\rm D}}^2\ + m_{\mathcal{P}}^2)^2 - 4m_{\mathcal{V}}^2 m_{\mathcal{P}}^2}}{(m_{\mathcal{V}}^2 - m_{\gamma^{\rm D}}^2\ )^3}\,. \tag{2}$$

For the branching ratios of the mesons to $\gamma\gamma$ or $\gamma\pi^0$, the same values as implemented in Pythia 8.2 were used. The average number of mesons produced per p.o.t., $\rm n_{meson}$ / p.o.t., is shown for each meson type in the last column, from toy samples of 100,000 proton-on-target (p.o.t.) non-diffractive collisions simulated with Pythia 8.230 [9]. The uncertainty is set to the mean deviation of the distributions obtained repeating the same simulations 1000 times.

$\rm m_{\gamma^D}$ (GeV)	meson	BR($\gamma + X$) [9]	$\rm n_{meson}$ / p.o.t.
0-0.135	$\pi^0 \to \gamma^{\rm D}\,\gamma$	0.98799	6.147 ± 0.003
0.135-0.548	$\eta \to \gamma^{\rm D}\,\gamma$	0.3931181	0.703 ± 0.008
0.548-0.648	$\omega \to \gamma^{\rm D}\,\pi^0$	0.0834941	0.825 ± 0.009
0.648-0.958	$\eta' \to \gamma^{\rm D}\,\gamma$	0.0219297	0.079 ± 0.003

Table 1: Meson decay modes considered for the $\gamma^{\rm D}$ production.

The cross section for the production of dark photon via meson decays produced in non-diffractive primary interactions of the proton beam is then computed as in equation 3, using equations 1 and 2 and values reported in table 1. The cross section is proportional to ε^2.

$$\sigma_{\text{meson}} = \frac{\sigma_{\text{pp}}^{\text{non-diff}}}{\sigma_{\text{pp}}^{\text{tot}}} \times n_{\text{meson}}/\text{p.o.t.} \times \text{Br}(\text{meson} \to \gamma^{\text{D}} + X)\,. \tag{3}$$

3.2 Production in proton bremsstrahlung

In analogy with ordinary photon bremsstrahlung of scattering protons, the same process is used for dark photon production by scattering of the incoming 400 GeV proton beam on the target protons. Following references [19, 16], the differential γ^{D} production cross section can be expressed as in equation 4:

$$\begin{aligned} \frac{dN}{dz dp_\perp^2} &= \frac{\sigma_{pp}(s')}{\sigma_{pp}(s)}\, w_{ba}(z, p_\perp^2)\,, \\ w_{ba}(z, p_\perp^2) &= \frac{\epsilon^2 \alpha_{QED}}{2\pi H}\left[\frac{1+(1-z)^2}{z} - 2z(1-z)\left(\frac{2m_p^2 + m_{\gamma^{\text{D}}}^2}{H} - z^2\frac{2m_p^4}{H^2}\right)\right. \\ &\quad \left. + 2z(1-z)\big(1+(1-z)^2\big)\frac{m_p^2 m_{\gamma^{\text{D}}}^2}{H^2} + 2z(1-z)^2\frac{m_{\gamma^{\text{D}}}^4}{H^2}\right]. \end{aligned} \tag{4}$$

where $\sigma_{pp}(s/s')$ are the inelastic proton-proton cross sections evaluated for the incoming/outgoing proton energy scales, m_p, P and E_p are the proton beam mass (set to $m_p = 0.938272081$ GeV/c [17]) and initial momentum and energy respectively, p and $E_{\gamma^{\text{D}}}$ are the momentum and energy of the generated dark photon respectively, $p_\perp$ and $p_\parallel$ are the components of the γ^{D} momentum orthogonal and parallel to the direction of the incoming proton respectively, α_{QED} is the fine structure constant of Quantum Electro Dynamic (QED), set to 1/137, $s' = 2m_p(E_p - E_{\gamma^{\text{D}}})$, $s = 2m_p E_p$ and $H(p_\perp^2, z) = p_\perp^2 + (1-z)m_{\gamma^{\text{D}}}^2 + z^2 m_p^2$.

However, the above formula does not take into account possible QCD contributions when the energy scale Q^2 of the process exceeds the QCD scale, and the bremsstrahlung process starts to depend on the internal partons. When the mass of the dark photon is much in excess of 1 GeV, the standard dipole form factor [20] is included in the proton-γ^{D} vertex, leading to a penalty factor that models the strong suppression of the bremsstrahlung production:

$$\text{penalty}(m_{\gamma^{\text{D}}}) = \left(\frac{m_{\gamma^{\text{D}}}^2}{0.71\,\text{GeV}^2}\right)^{-4} \quad \text{for} \quad m_{\gamma^{\text{D}}}^2 > 0.71\,\text{GeV}^2, \tag{5}$$

According to reference [16], this form factor is conservative and probably underestimates the rates. As we are however considering direct parton-parton QCD production in section 3.3, to avoid double-counting this conservative option is adopted.

The inelastic proton-proton cross section $\sigma_{pp}(s)$ is taken from experimental data:

$$\sigma_{pp}(s) = Z + B \cdot \log^2\left(\frac{s}{s_0}\right) + Y_1\left(\frac{s_1}{s}\right)^{\eta_1} - Y_2\left(\frac{s_1}{s}\right)^{\eta_2}, \tag{6}$$

where $Z = 35.45$ mb, $B = 0.308$ mb, $Y_1 = 42.53$ mb, $Y_2 = 33.34$ mb, $\sqrt{s_0} = 5.38$ GeV, $\sqrt{s_1} = 1$ GeV, $\eta_1 = 0.458$ and $\eta_2 = 0.545$ [21].

Reformulating equation 4 as a function of the γ^{D} angle θ to the beam line and its total momentum p, a two-dimensional normalised probability density function (PDF) $f(p, \theta)$ is extracted, and shown in figure 1 for two choices of $\text{m}_{\gamma^{\text{D}}}$. Note that due to the simple dependency

of the production rate scaling as ε^2, the normalised PDF is independent of ε. The dark photons are generated with maximum probability on each side of the beam axis (θ close to 0) with a factor of 5 more chance to have p$<$ 100 GeV compared to p$>$ 200 GeV, for the low masses, and increased probability to have high momentum as the mass increases, with the highest probability to have the maximum momentum available for $m_{\gamma^D} = 2$ GeV.

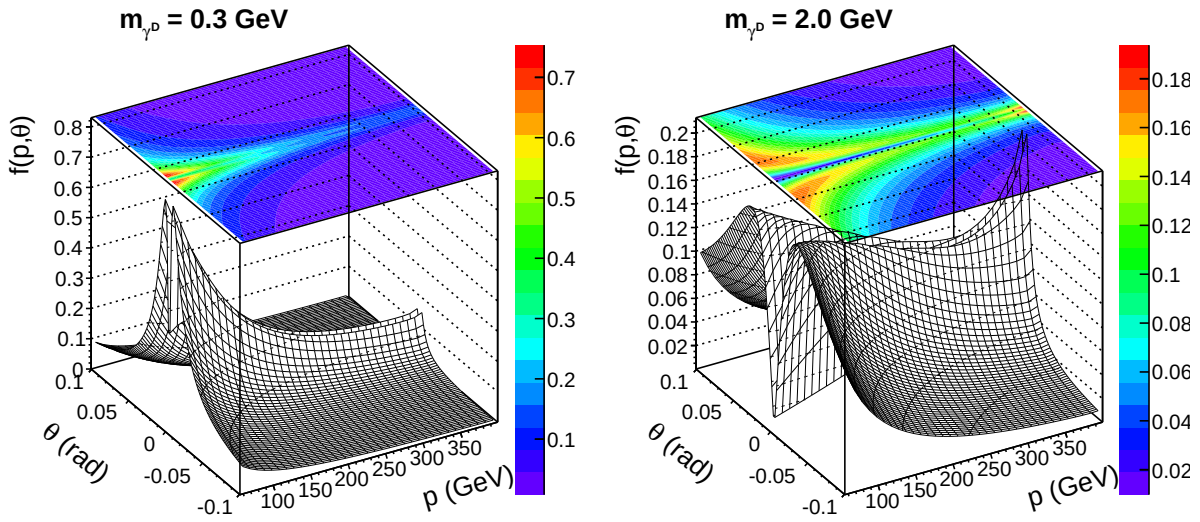

Figure 1: Normalised probability density function of producing a dark photon with angle θ and momentum p through proton bremsstrahlung, for two examples of m_{γ^D} : 0.3 GeV (left) and 2 GeV (right).

Events are generated using the Pythia8 gun with the γ^D as particle, randomly choosing the γ^D (p, θ) values according to the normalised 2D PDF $f(p, \theta)$, extracted for each m_{γ^D} point studied.

The integral of $f \times \text{penalty}(m_{\gamma^D})$ in the kinematically allowed range of momenta, and complete solid angle $\theta(-\pi/2, \pi/2)$, provides an estimate of the total dark photon production rate σ_{pbrem} through proton bremsstrahlung, scaling as ε^2. The conditions of validity of the approximation used to derive equation 4 [22, 23] require a lower momentum bound for the γ^D at $p_{min} = 0.14 P_p$ [19], the upper bound being given by the incoming 400 GeV proton beam and m_{γ^D} .

3.3 Drell-Yan production

For production of the dark photon in parton-parton scattering, the generic implementation of a resonance that couples both to SM fermion pairs and hidden particles is used, as implemented in Pythia 8.2 under the "HiddenValley" Z' model [24]. A cross-check has been done that similar kinematic distributions for the dark photons are found using another Z' implementation in Pythia from the "New Gauge Bosons" class of processes [25].

The dark photons are generated in the mass range $1.4 < m_{\gamma^D} < 10$ GeV. Below 1.4 GeV one leaves the domain of perturbative QCD and the parton model cannot be used anymore.

The cross section given by Pythia when the new particle has the properties of the dark photon is shown in figure 2. Like for the meson and proton bremsstrahlung processes, it is found to scale as ε^2. An empirical function is extracted to parametrise the cross section as a function of the γ^D mass in a continuous way, described in equation 7.

$$
\begin{aligned}
1.4 < \mathrm{m}_{\gamma^{\mathrm{D}}} &\leq 3\,\mathrm{GeV} : \sigma_{\mathrm{QCD}} = \varepsilon^2 \times e^{-4.1477-1.4745\times \mathrm{m}_{\gamma^{\mathrm{D}}}} \quad , \\
\mathrm{m}_{\gamma^{\mathrm{D}}} &> 3\,\mathrm{GeV} : \sigma_{\mathrm{QCD}} = \varepsilon^2 \times e^{-5.928-0.8669\times \mathrm{m}_{\gamma^{\mathrm{D}}}} \quad .
\end{aligned}
\tag{7}
$$

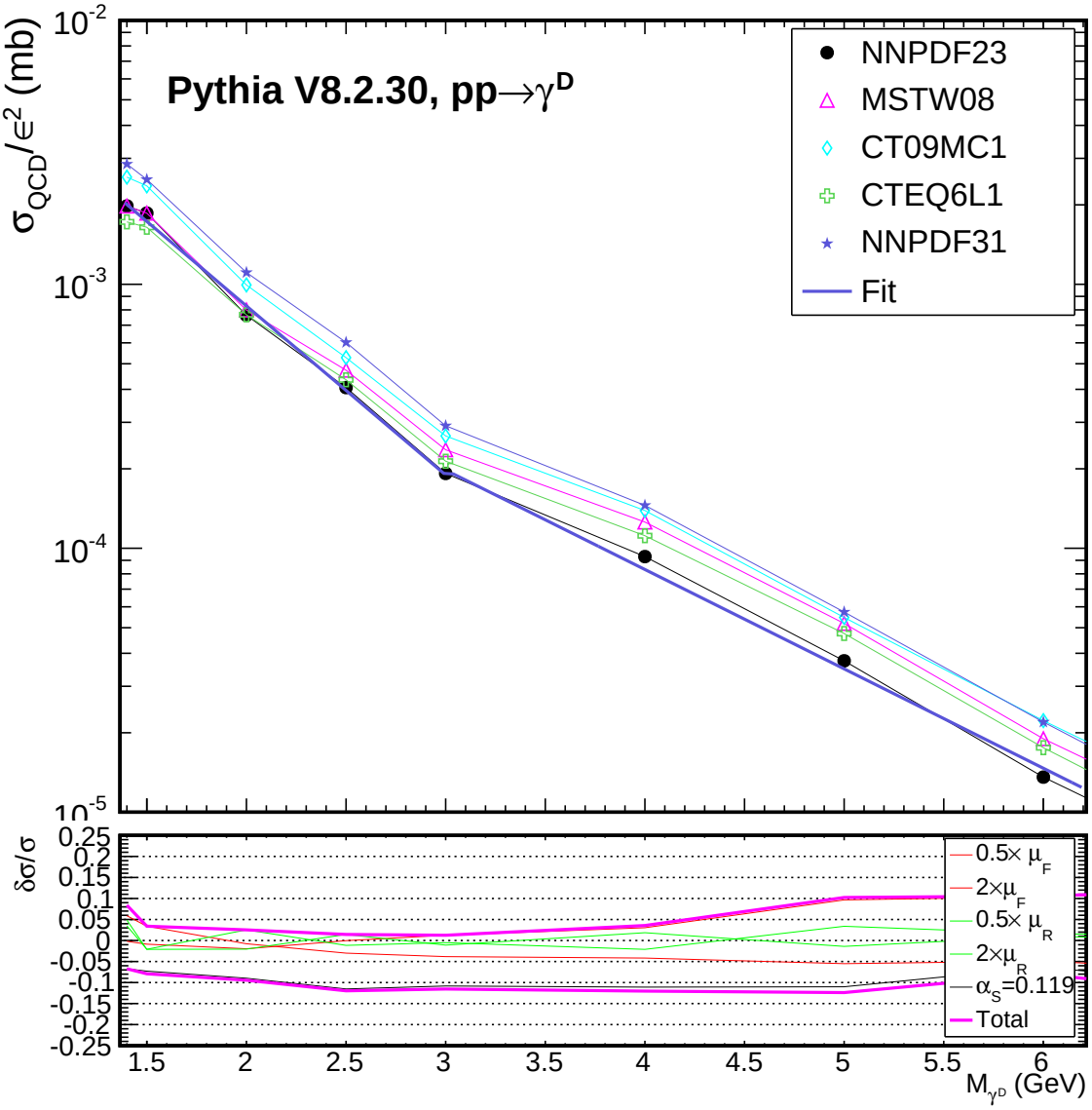

Figure 2: QCD production cross section as a function of $\mathrm{m}_{\gamma^{\mathrm{D}}}$. The fit function is described in equation 7. The lower pad shows the relative uncertainties from several theoretical uncertainty sources on the cross section calculated by Pythia.

The relative contribution from each process is shown in figure 3, as a function of $\mathrm{m}_{\gamma^{\mathrm{D}}}$, for the three production modes.

3.4 Dark photon decays

Except for the meson production mode, in which the new particle couples to the parent meson via mixing with the photon and hence cannot be a resonance from Pythia's point-of-view, in QCD and proton bremsstrahlung the γ^{D} is made a proper resonance. In all cases, the decay modes are implemented by hand as follows.

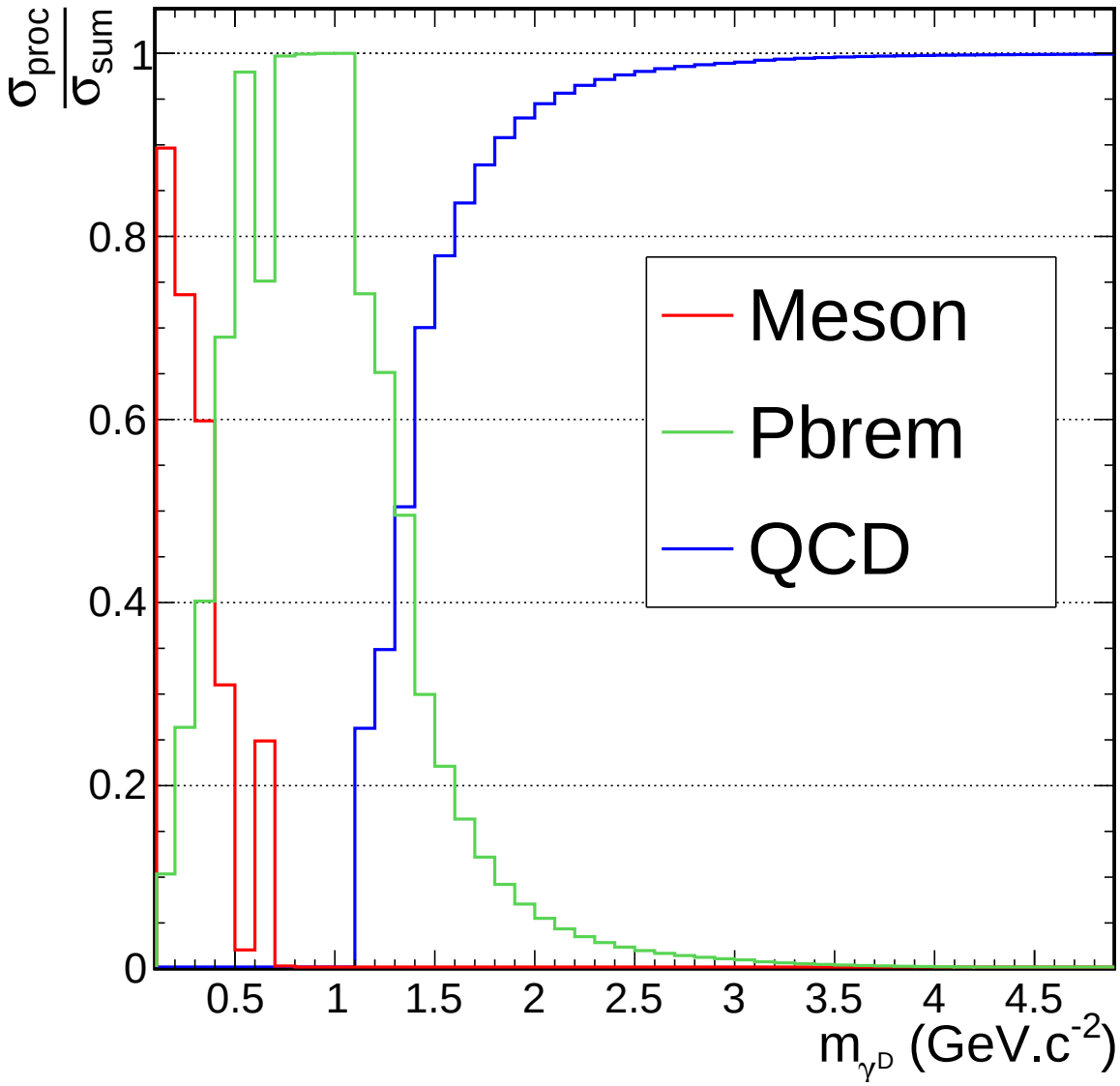

Figure 3: Relative contributions to the cross section as a function of m_{γ^D} for the three production modes studied.

The partial decay width of the dark photon into a lepton pair is given by [19]:

$$\Gamma(\gamma^{\mathrm{D}} \rightarrow l^+l^-) = \frac{1}{3}\alpha_{\mathrm{QED}} m_{\gamma^{\mathrm{D}}}\, \epsilon^2 \sqrt{1 - \frac{4m_l^2}{m_{\gamma^{\mathrm{D}}}^2}} \left(1 + \frac{2m_l^2}{m_{\gamma^{\mathrm{D}}}^2}\right) , \tag{8}$$

where m_l is the lepton mass, for electron, muon or tau leptons, if kinematically allowed. Following the approach used by the authors of [26], the partial decay width into quark pairs is computed as:

$$\Gamma(\gamma^{\mathrm{D}} \rightarrow \text{ hadrons}) = \frac{1}{3}\alpha_{\mathrm{QED}} m_{\gamma^{\mathrm{D}}}\, \epsilon^2 R\left(m_{\gamma^{\mathrm{D}}}\right) , \tag{9}$$

where

$$R\left(\sqrt{s}\right) = \frac{\sigma(e^+e^- \rightarrow hadrons)}{\sigma(e^+e^- \rightarrow \mu^+\mu^-)} \tag{10}$$

is the energy-dependent R-ratio quantifying the hadronic annihilation in e^+e^- collisions [21], tabulated from 0.3 to 10.29 GeV.

The lifetime of the γ^D is then naturally set to the inverse of its total width, summing all the kinematically-allowed channels in calculating the total width. It is proportional to $1/\varepsilon^2$. The branching ratios to individual channels are set to the ratio of the partial over total width, and are hence independent of ε. For separating the hadronic channels into the different quark-flavoured pairs, the same relative branching ratios as those of the SM Z bosons are used, namely: 0.22031, 0.17089, 0.22029, 0.17066, 0.21785 for decays to $u\bar{u}$, $d\bar{d}$, $s\bar{s}$, $c\bar{c}$, $b\bar{b}$, respectively [9]. When the γ^D is a resonance, the decay goes explicitly through the pair of quarks, before hadronisation. However in the case of the meson production, the hadrons are found as direct decay products of the γ^D .

The branching ratio of the γ^D into the different final states is shown in figure 4 as a function of m_{γ^D} . The hadronic decays become available above the pion mass threshold. The expected lifetime of the γ^D as a function of its mass and ε mixing parameter is shown in figure 5.

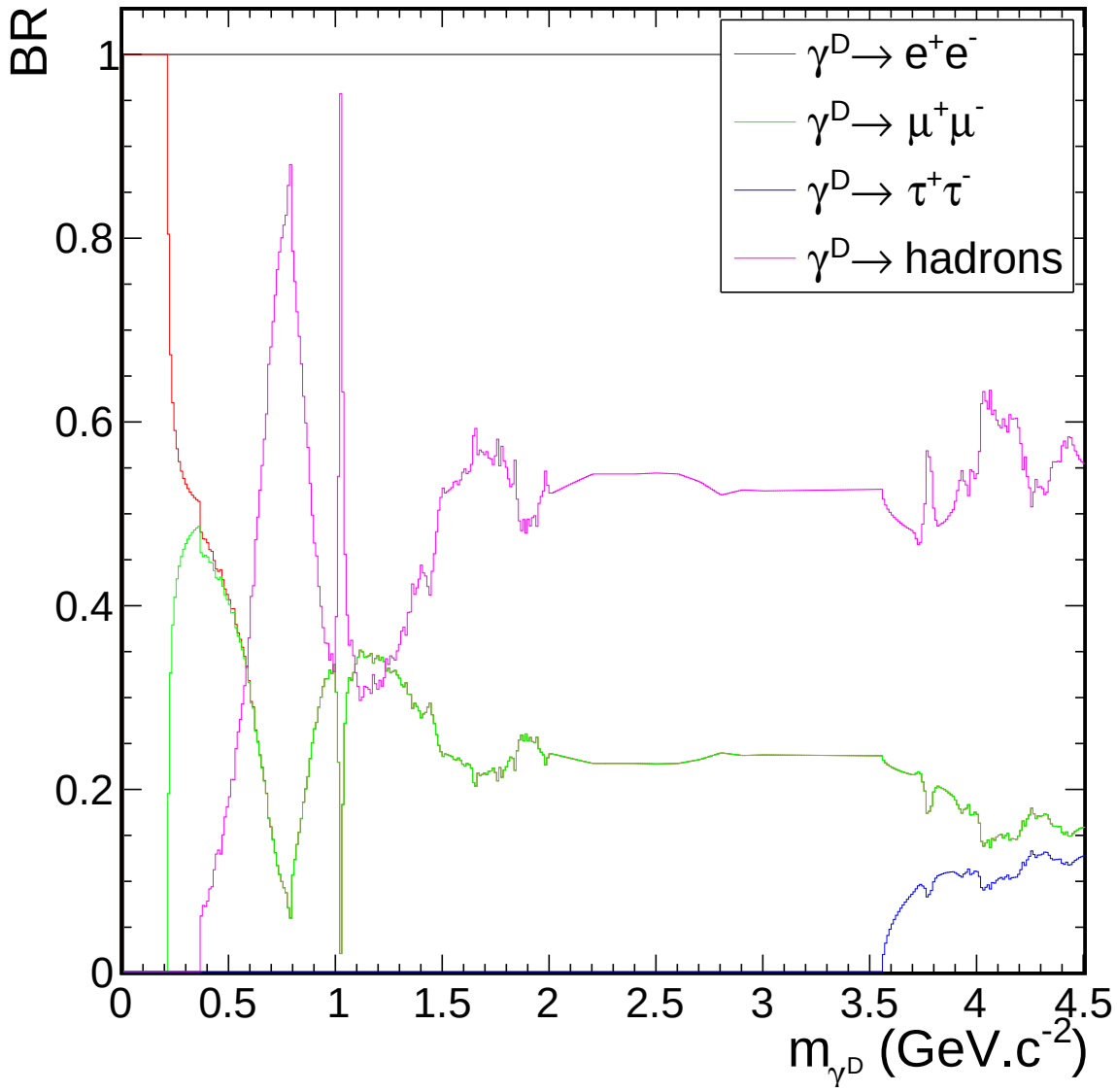

Figure 4: Branching ratio of the γ^D into fermion pairs as a function of its mass.

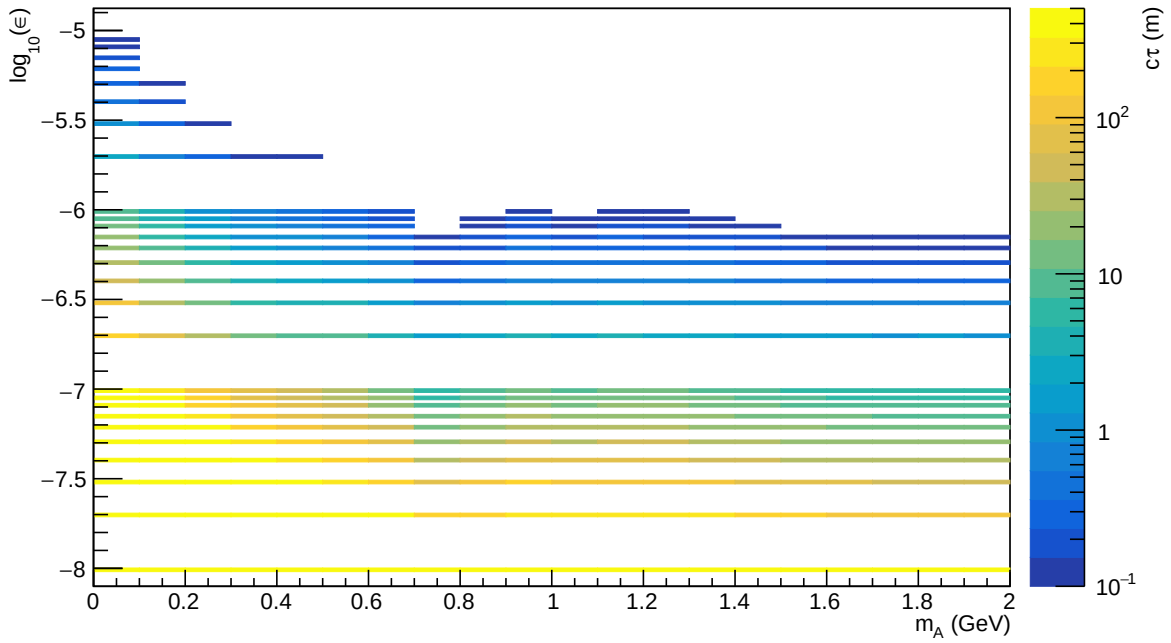

Figure 5: Expected lifetime of the dark photon as a function of its mass and of the kinetic mixing parameter ε.

4 SHiP sensitivity

In order to maximise the usability of the events produced by Pythia in the different production modes, the γ^{D} decay vertex position is randomly assigned to be inside the decay vessel of length $\mathrm{L_{Vessel}} = 50.760\,\mathrm{m}$, and the associated probability of this happening is given as a function of the γ^{D} quadrivector (p, $\mathrm{E}_{\gamma^{\mathrm{D}}}$) and lifetime $\mathrm{c}\tau$ by equation 11.

$$\mathrm{w_{vtx}}(\ell) = e^{\frac{-\ell}{\beta\times\gamma\times\mathrm{c}\tau}} \times \frac{\mathrm{L_{Vessel}}}{\beta\times\gamma\times\mathrm{c}\tau}\,, \tag{11}$$

with $\gamma = E_{\gamma^{\mathrm{D}}}\,/\sqrt{E^2_{\gamma^{\mathrm{D}}} - p^2}$, $\beta = p/E_{\gamma^{\mathrm{D}}}$ and ℓ randomly distributed between 0 and $\mathrm{L_{Vessel}}$ with a flat prior.

The total event rate expected is then expressed in equation 12, for each production mode m (meson, proton bremsstrahlung, QCD):

$$n(\gamma^{\mathrm{D}}\,|\mathrm{m}) = \mathrm{N\,(p.o.t.)} \times \sigma_{\mathrm{m}}(pp \to \gamma^{\mathrm{D}}\,) \times \int_{\mathrm{Vessel}} \mathrm{w_{vtx}}(\ell)\mathrm{d}\ell \times \mathcal{A}_{\mathrm{det}}\,, \tag{12}$$

$\mathrm{N\,(p.o.t.)} = 2\times10^{20}$ is the total number of p.o.t. expected by the end of the SHiP physics program, and $\mathcal{A}_{\mathrm{det}}$ is the detector acceptance times efficiency to reconstruct the decay products in the SHiP detector and is described in detail in section 4.3.

The strategy of the analysis relies on identifying the decays of the γ^{D} into at least two charged particles. The reconstructed charged tracks must originate from a common vertex. These requirements are enough to ensure that no background event will survive the selection, as demonstrated in [7, 27]. The 90% confidence level (CL) limits on the existence of a γ^{D} with given ($\mathrm{m}_{\gamma^{\mathrm{D}}}$, ε) are hence set by excluding regions where more than 2.3 events are expected.

4.1 Decay modes

The following decay modes are considered, whenever available according to m_{γ^D} : e^+e^-, $\mu^+\mu^-$, $\tau^+\tau^-$ in one-prong decay modes, and any other hadronic decay modes leading to two charged particles (e.g. $\pi^+\pi^- + X$, $K^+K^- + X$). The branching ratio to the different decay modes is shown in figure 6 for all the simulated (m_{γ^D} , ε) points in the three different production modes, as a function of m_{γ^D} , calculating the mean value over the different ε samples.

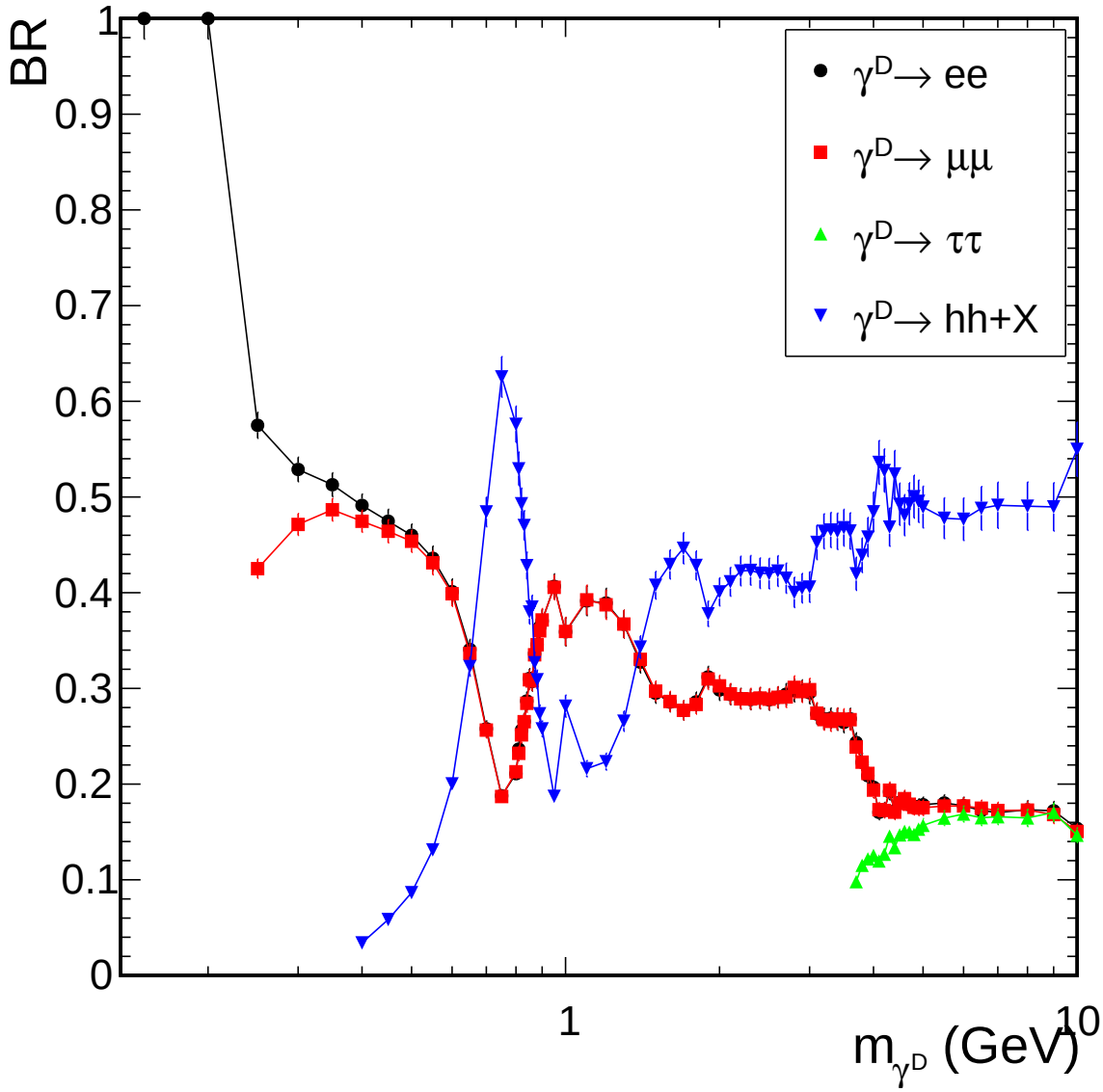

Figure 6: Branching ratio to the visible decay channels producing two charged particles, as a function of m_{γ^D} .

4.2 Vessel acceptance

For events which have two charged particles, the γ^D decay vertex is further required to be within the vessel volume. The efficiency of this selection is shown in figure 7 as a function of (m_{γ^D} , ε), for the three production modes. This efficiency is mostly driven by the lifetime of the γ^D , and the kinematics of the γ^D produced in the target. It is around 5% for meson and proton bremstrahlung productions, and reaches 10% for higher masses in QCD production.

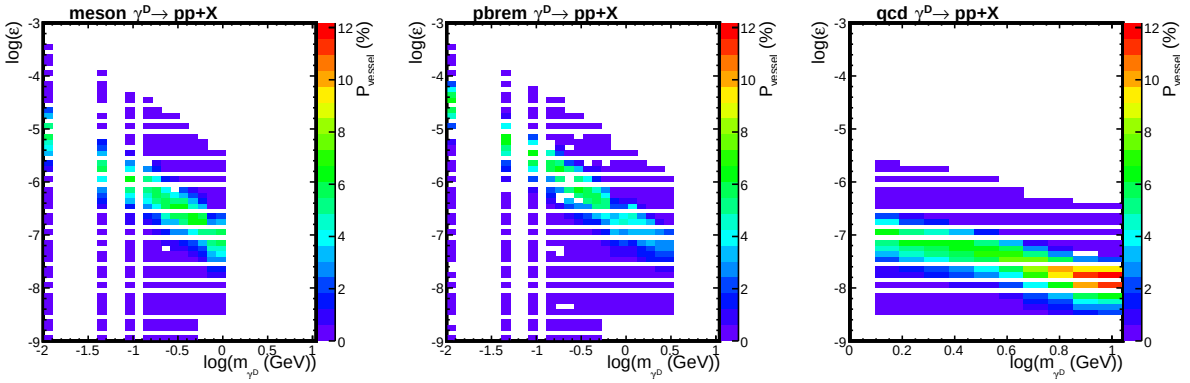

Figure 7: Efficiency of requiring the γ^{D} decay vertex to be inside the decay vessel volume.

4.3 Reconstruction of the decay products

The strategy employed in this analysis relies uniquely on the reconstruction of charged particles by the SHiP straw tracker. Future extensions of this work could consider also calorimeter deposits (to tag e.g. photons from π^0 decays) and muon detectors. Events are retained if two tracks are found passing the criteria summarised in table 2, namely that the two tracks are within the fiducial area of the detector up to the fourth layer after the magnet, the fit converged with good quality requirements, they have impact parameters less than 0.1 m in the (x,y) plane and a momentum above 1 GeV. Criteria on the number of hits (NDF>25) or presence of hits before/after the magnet are meant to reduce backgrounds which could come from particles re-entering the detector volume due to the magnetic field.

Decay vertex	z between straw veto tagger and exit lid of vacuum vessel (1 m) x-y within vessel volume (± 5 cm)
Straw tracker hits	in each layer - before and after magnet - up to station 4
Tracks	NDF > 25, $\chi^2/NDF < 5$, doca < 1 cm >=2 tracks p$>$ 1 GeV, IP$<$ 0.1 m

Table 2: Selection criteria applied on the reconstructed events.

The efficiency of having two good tracks passing the selection for events which had two charged particles and γ^{D} vertex in the decay volume is shown in figure 8. Once the γ^{D} decays in the volume, the reconstruction efficiency is above 80% in most of the parameter space. For production via meson decay, a dependency on ε is observed, with the efficiency dropping to below 50% as ε decreases.

4.4 Systematic uncertainties

The following sources of systematic uncertainties from theory are investigated, for the three modes. They concern only the overall normalisation, and not the impact from modifying the shapes of the γ^{D} kinematic variables, for which we rely on Pythia 8 (for meson and QCD production) or available theoretical assumptions for the proton bremsstrahlung production as described in section 3.2. The missing contributions from cascade decays will be the subject of future work and is not considered.

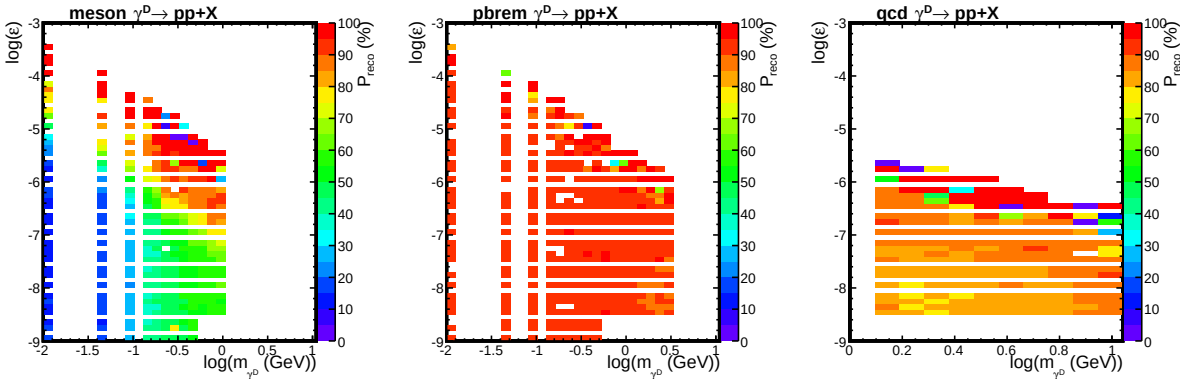

Figure 8: Efficiency of requiring two good tracks, for events with two charged particles and γ^{D} vertex inside the vessel volume.

For the meson production, the overall rate is affected by the following uncertainties:

- which meson is chosen to give the kinematical properties of the event: first encountered, last (central choice up to now), random. Because only one meson channel per mass range is considered, the impact is expected to be relevant only for the lower masses. @TODO: evaluate impact plotting (p,theta) PDF from primary interactions.
- Branching ratios from table 1: from [17], the uncertainties on the measurement of these branching ratios are 0.03%, 0.5%, 3.4% and 3.6% for $\pi^0 \to \gamma\gamma$, $\eta^0 \to \gamma\gamma$, $\omega \to \pi^0\gamma$ and $\eta' \to \gamma\gamma$ respectively, translating directly to the final rate.
- Uncertainty on $\mathrm{n_{meson}}$ / p.o.t.: from Pythia 8, as detailed in section 3.1 and table 1, they amount to 0.05%, 1.1%, 1.1% and 3.8% for π^0, η^0, ω and η' respectively, also translating directly to the final rate.
- Uncertainty on $\frac{\sigma_{\mathrm{pp}}^{\mathrm{non-diff}}}{\sigma_{\mathrm{pp}}^{\mathrm{tot}}}$: the uncertainty on $\sigma_{\mathrm{pp}}^{\mathrm{tot}}$ is 3%. A conservative 5% is taken on the ratio, translating directly to the final rate.
- Theory uncertainties on branching ratio of mesons to dark photons: ??

Adding the different sources in quadrature, this results in a total systematic uncertainty of $\pm 5 - 7\%$ depending on the mass.

For the proton bremsstrahlung, the theory systematic uncertainties concern:

- uncertainties on the inelastic proton-proton cross section $\sigma_{pp}(s)$ will mostly cancel in the ratio $\frac{\sigma_{pp}(s')}{\sigma_{pp}(s)}$ so are neglected.
- Dipole form-factor.
- Uncertainty on w_{ba}: ??
- Lower bound on p: ?

A total systematic uncertainty of $\pm 20\%$ is assumed to cover these sources.

For the QCD production, the theory systematic uncertainties concern the parametrisation of the cross section, and impact from QCD scales and PDFs. Figure 2 shows the relative contributions from QCD scales and PDF. The choice of PDF set is not taken as a systematic uncertainty, given the large variations observed which are nevertheless not affecting the overall shape of the

cross section versus mass. Adding the different sources in quadrature, this results in a conservative total systematic uncertainty of $^{+5\%}_{-10\%}$.

Experimental systematic uncertainties concern:

- modelling of the tracking efficiency,
- 0-background assumption.

They have been neglected in this study, expected to be small compared to the theoretical uncertainties.

4.5 Extraction of the limit

Events are generated following a discrete grid in (m_{γ^D} ,ε) values, and passed through the full simulation of the SHiP detector and reconstruction algorithms. To find the ε value(s) that allow to reach 2.3 expected events, the expected rate is studied as a function of ε for discrete mass points, with a linear interpolation between fully-simulated values. Between mass points, a linear interpolation is also done. The rate of events is driven by two aspects: for large ε values, larger cross sections are expected but the events are suppressed due to small lifetimes and decays happening before the decay vessel. As ε decreases, the cross section decreases as ε^2 but the events have more and more probability to reach the vessel and the rate increases, up to a turn-on point where the decay vertex happens after the decay vessel and/or the cross section becomes too small. Hence the 90% CL exclusion region is contained inside a lower and upper limits on ε^2 for each mass point. The dependency of the excluded region on the mass is driven by the kinematic properties of the γ^D and its daughters, affecting the detector acceptance and selection efficiency.

As shown in figure 9 for representative mass points, for meson and proton bremsstrahlung processes, the bounds have very little dependency on the absolute normalisation of the rate (so in particular systematic uncertainties on the cross sections and other quantities affecting the overall rate), due to the very steep dependency of the rate as a function of ε. However, for the QCD production, the behaviour is flatter and 5% increase in rate leads to an extra 0.1 GeV in sensitivity.

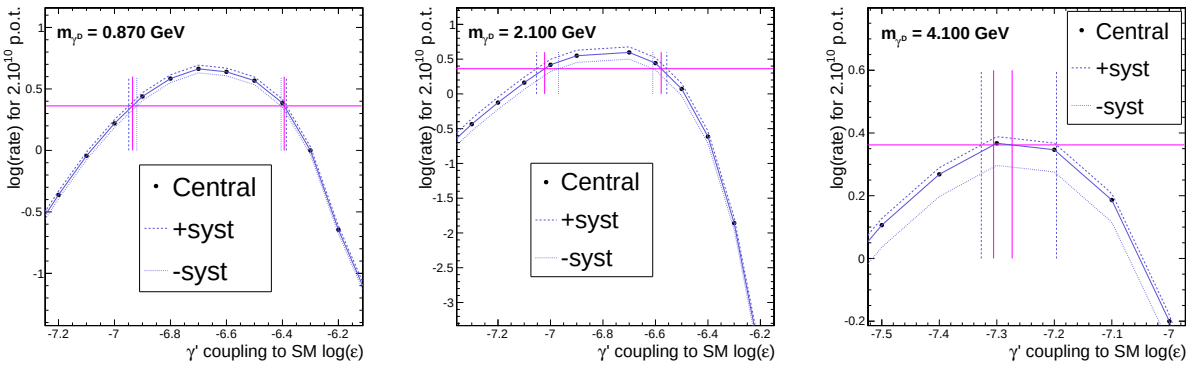

Figure 9: Expected rate as a function of ε, for $m_{\gamma^D} = 0.87$ (left), 2.1 (middle) or 4.1 (right) GeV and meson, proton bremsstrahlung or QCD production, respectively.

The 90% CL exclusion contours are shown in figure 10 for the three production mode studied, in the (m_{γ^D} ,ε) plane, with the impact from systematic uncertainties.

The 90% CL exclusion contour is shown in figure 11 for the three production mode studied, in the (m_{γ^D} ,ε) plane. Exclusion contours from theoretical constraints, existing and other

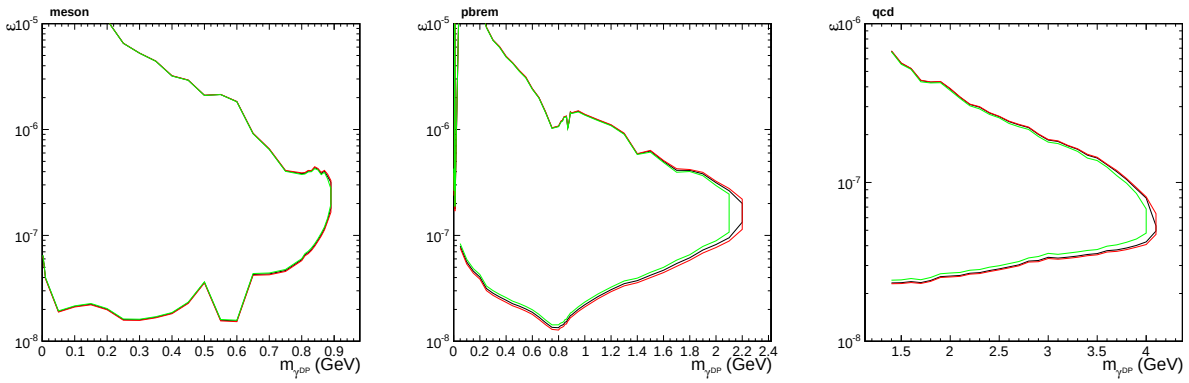

Figure 10: Expected 90% exclusion region as a function of the dark photon mass and of the kinetic mixing parameter ε, for the three production modes studied. Systematic variations are shown with red and green lines.

planned experiments sensitive to this process are overlayed. The SHiP experiment is found to have a unique sensitivity in the mass region m_{γ^D} ranging between XX and XX GeV, and ε ranging between XX and XX.

An alternative scenario in which the γ^D would couple only to leptons is also considered ("leptophilic" case) and exclusion contour shown in figure 12.

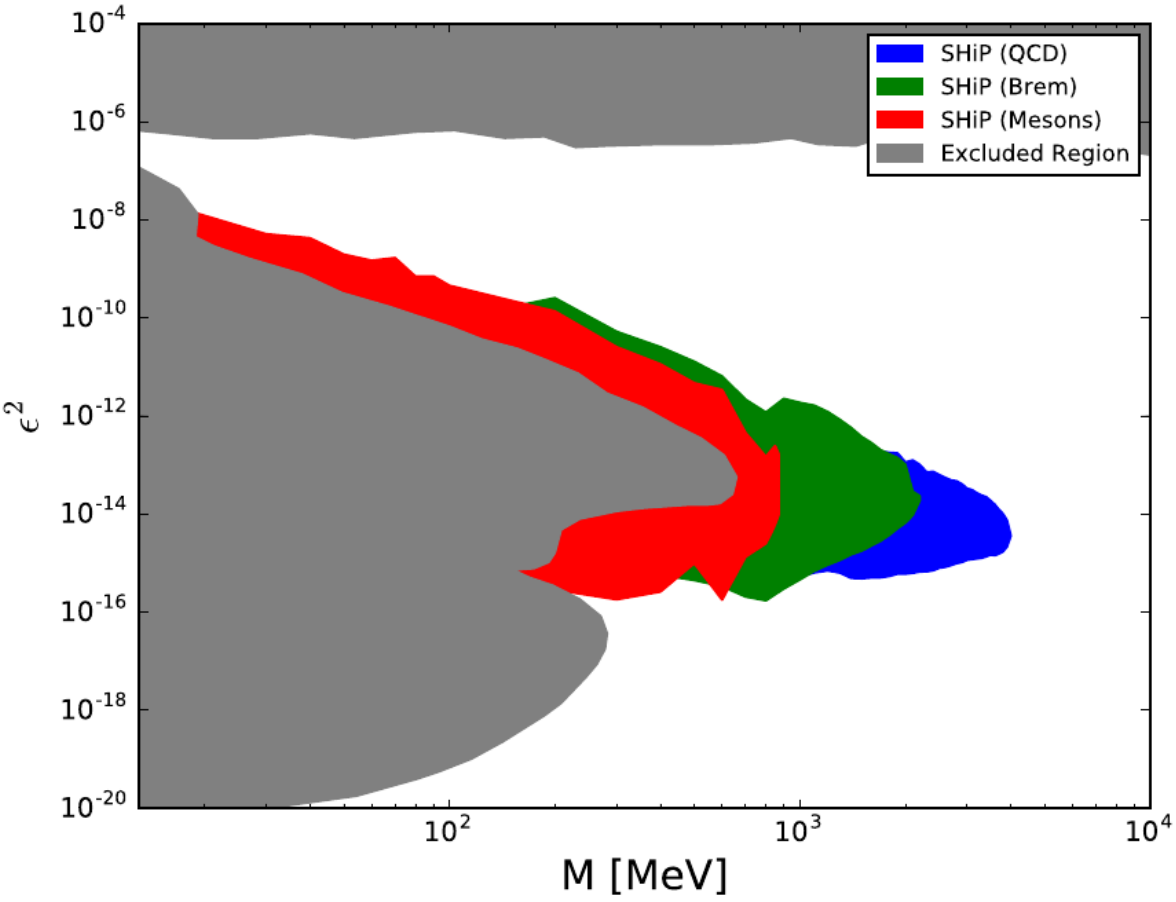

Figure 11: Expected 90% exclusion region as a function of the dark photon mass and of the kinetic mixing parameter ε, for the three production modes studied.

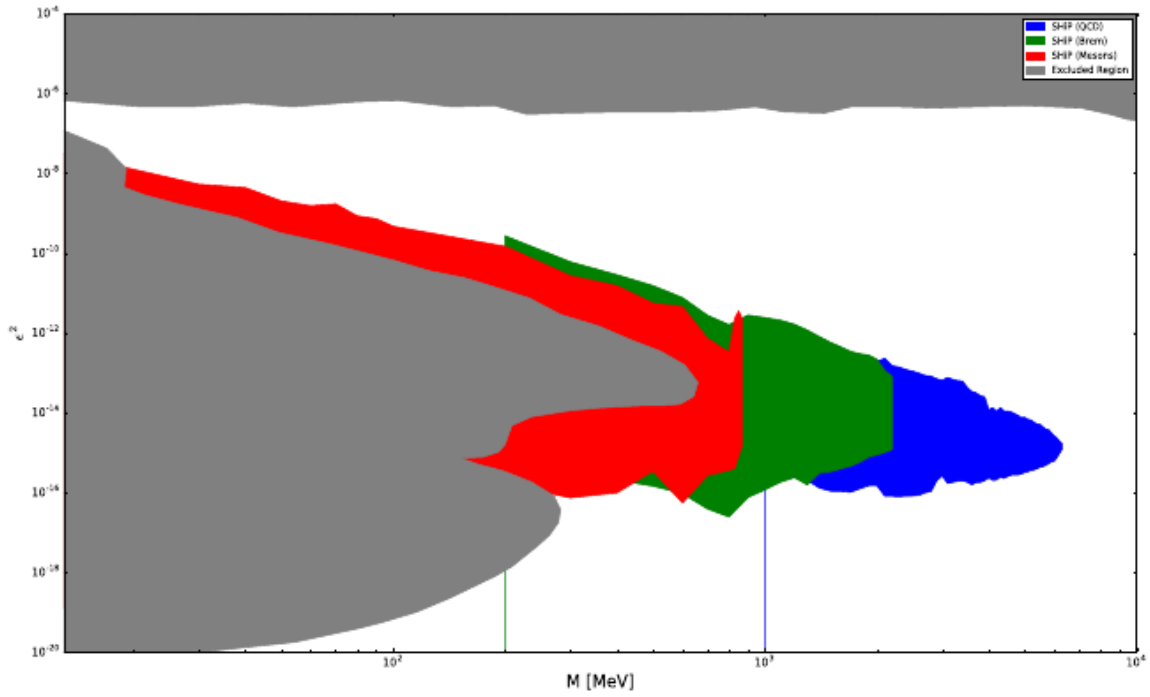

Figure 12: Expected 90% exclusion region as a function of the dark photon mass and of the kinetic mixing parameter ε, for the three production modes studied, in scenarios where the γ^{D} couples only to standard model leptons.

5 Conclusion

The sensitivity of the SHiP detector has been investigated for the simplest vector portal model, whereby the only hidden-sector particle connecting to SM particles is a dark photon. The model is fully parametrised by only two parameters, the mass of the dark photon $m_{\gamma^{\mathrm{D}}}$ and the kinetic mixing parameter ε. Three different production mechanisms have been investigated, namely the production via meson decays from non-diffractive proton-proton interactions, by proton bremsstrahlung and by QCD parton-parton interaction. Only the primary proton-proton interaction is taken into account, secondaries from hadronic interactions in cascade decays could lead to additional sensitivity and will be the object of future work. The dark photon is assumed to decay to pairs of fermions, and only decay channels producing at least two charged particles coming from a common vertex are used. With the selection applied, no background event is expected and 90% CL exclusion contours are extracted and compared with those from theoretical constraints and other existing or planned experiments. The SHiP detector is expected to have a unique sensitivity for $m_{\gamma^{\mathrm{D}}}$ ranging between XX and XX GeV, and ε ranging between XX and XX.

References

[1] L. Evans and P. Bryant, "LHC Machine," *JINST*, vol. 3, p. S08001, 2008.

[2] G. Apollinari, I. Béjar Alonso, O. Brüning, M. Lamont, and L. Rossi, "High-Luminosity Large Hadron Collider (HL-LHC) : Preliminary Design Report," 2015.

[3] M. Aaboud *et al.*, "Search for Higgs boson decays to beyond-the-Standard-Model light bosons in four-lepton events with the ATLAS detector at $\sqrt{s} = 13$ TeV," *JHEP*, vol. 06, p. 166, 2018.

[4] M. Aaboud *et al.*, "Search for new high-mass phenomena in the dilepton final state using 36 fb^{-1} of proton-proton collision data at $\sqrt{s} = 13$ TeV with the ATLAS detector," *JHEP*, vol. 10, p. 182, 2017.

[5] "A search for pair production of new light bosons decaying into muons at sqrt(s)=13 TeV," Tech. Rep. CMS-PAS-HIG-18-003, CERN, Geneva, 2018.

[6] V. Khachatryan *et al.*, "Search for narrow resonances in dilepton mass spectra in proton-proton collisions at $\sqrt{s}$ = 13 TeV and combination with 8 TeV data," *Phys. Lett.*, vol. B768, pp. 57–80, 2017.

[7] M. Anelli *et al.*, "A facility to Search for Hidden Particles (SHiP) at the CERN SPS," 2015.

[8] M. Anelli *et al.*, "Sensitivity of the SHiP experiment to Heavy Neutral Leptons," 2018.

[9] T. Sjöstrand, S. Ask, J. R. Christiansen, R. Corke, N. Desai, P. Ilten, S. Mrenna, S. Prestel, C. O. Rasmussen, and P. Z. Skands, "An Introduction to PYTHIA 8.2," *Comput. Phys. Commun.*, vol. 191, pp. 159–177, 2015.

[10] C. Andreopoulos *et al.*, "The GENIE Neutrino Monte Carlo Generator," *Nucl. Instrum. Meth.*, vol. A614, pp. 87–104, 2010.

[11] T. Sjöstrand, S. Mrenna, and P. Z. Skands, "Pythia 6.4 physics and manual," *Journal of High Energy Physics*, vol. 2006, no. 05, p. 026, 2006.

[12] "Heavy Flavour Cascade Production in a Beam Dump," Dec 2015.

[13] S. Agostinelli *et al.*, "GEANT4: A Simulation toolkit," *Nucl. Instrum. Meth.*, vol. A506, p. 250, 2003.

[14] M. Al-Turany, D. Bertini, R. Karabowicz, D. Kresan, P. Malzacher, T. Stockmanns, and F. Uhlig, "The fairroot framework," *Journal of Physics: Conference Series*, vol. 396, no. 2, p. 022001, 2012.

[15] B. Holdom, "Two U(1)'s and Epsilon Charge Shifts," *Phys. Lett.*, vol. 166B, pp. 196–198, 1986.

[16] D. Gorbunov, A. Makarov, and I. Timiryasov, "Decaying light particles in the SHiP experiment: Signal rate estimates for hidden photons," *Phys. Rev.*, vol. D91, no. 3, p. 035027, 2015.

[17] C. Patrignani *et al.*, "Review of Particle Physics," *Chin. Phys.*, vol. C40, no. 10, p. 100001, 2016.

[18] B. Batell, M. Pospelov, and A. Ritz, "Exploring Portals to a Hidden Sector Through Fixed Targets," *Phys. Rev.*, vol. D80, p. 095024, 2009.

[19] J. Blümlein and J. Brunner, "New Exclusion Limits on Dark Gauge Forces from Proton Bremsstrahlung in Beam-Dump Data," *Phys. Lett.*, vol. B731, pp. 320–326, 2014.

[20] L. N. Hand, D. G. Miller, and R. Wilson, "Electric and magnetic form factors of the nucleon," *Rev. Mod. Phys.*, vol. 35, pp. 335–349, Apr 1963.

[21] K. A. Olive *et al.*, "Review of Particle Physics," *Chin. Phys.*, vol. C38, p. 090001, 2014.

[22] K. Kim and Y. Tsai, "An improved weizsacker williams method and photoproduction of lepton pairs," *Physics Letters B*, vol. 40, no. 6, pp. 665 – 670, 1972.

[23] K. Kim and Y.-. Tsai, "Improved weizsaecker–williams method and its application to lepton and w- boson pair production," *Phys. Rev., D, v. 8, no. 9, pp. 3109-3125*, Nov 1973.

[24] L. Carloni, J. Rathsman, and T. Sjostrand, "Discerning Secluded Sector gauge structures," *JHEP*, vol. 04, p. 091, 2011.

[25] C. Ciobanu, T. Junk, G. Veramendi, J. Lee, G. De Lentdecker, K. S. McFarland, and K. Maeshima, "Z' generation with PYTHIA," 2005.

[26] J. D. Bjorken, R. Essig, P. Schuster, and N. Toro, "New Fixed-Target Experiments to Search for Dark Gauge Forces," *Phys. Rev.*, vol. D80, p. 075018, 2009.

[27] S. Alekhin *et al.*, "A facility to Search for Hidden Particles at the CERN SPS: the SHiP physics case," 2015.